A EUROPEAN JOURNAL OF CHEMICAL BIOLOGY

CHEMBIOCHEM

SYNTHETIC BIOLOGY & BIO-NANOTECHNOLOGY

Accepted Article

Title: Structure and substrate recognition of the Bottromycin maturation enzyme BotP

Authors: Greg Mann; Liujie Huo; Sebastian Adam; Brunello Nardone; Jeremie Vendome; Nicholas James Westwood; Rolf Müller; Jesko Koehnke

To be cited as: ChemBioChem 10.1002/cbic.201600406

Link to VoR: http://dx.doi.org/10.1002/cbic.201600406

A Journal of

ChemPubSoc Europe

www.chembiochem.org

WILEY-VCH

FULL PAPER WILEY-VCH

Structure and substrate recognition of the Bottromycin maturation enzyme BotP

Greg Mann,[a, +] Liujie Huo,[b, +] Sebastian Adam,[c] Brunello Nardone,[a] Jeremie Vendome,[d, e] Nicholas James Westwood,[a] Rolf Müller,[f] Jesko Koehnke*[c]

Abstract: The bottromycins are a family of highly modified peptide natural products displaying potent antimicrobial activity against Gram-positive bacteria including methicillin-resistant *Staphyloccoccus aureus*. Bottromycins have recently been shown to be ribosomally synthesized and post-translationally modified peptides (RiPPs). Uniquely amongst RiPPs the precursor peptide BotA contains a C-terminal follower, rather than the canonical N-terminal leader sequence. We report the structural and biochemical characterization of BotP, a leucyl-aminopeptidase like enzyme from the bottromycin pathway. We demonstrate that BotP is responsible for the removal of the N-terminal methionine from the precursor peptide. The crystal structures of apo BotP and of BotP in complex with Mn^{2+} allowed us to model a BotP/substrate complex and to rationalize substrate recognition. Our data represent the first step towards targeted compound modification to unlock the full antibiotic potential of bottromycin.

Introduction

Bottromycins have recently been identified as ribosomally synthesized and post-translationally modified peptides (RiPPs) – a growing class of natural products[1]. Like other RiPPs, bottromycins are derived from a core peptide, which is part of a larger precursor peptide (BotA). It is encoded for by a structural gene, which undergoes extensive post-translational modifications (PTMs) by a series of enzymes to become the final product[1] (Figure 1). Uniquely amongst RiPPs, BotA contains a C-terminal follower sequence, in place of an N-terminal leader sequence, which is thought to be important for stability and recognition of PTM enzymes[1,2]. The genes responsible for bottromycin biosynthesis, including that of the precursor peptide (*botA*) and the necessary tailoring enzymes, are localized within a single biosynthetic gene cluster[3,4] (Figure 1). Bottromycin maturation involves multiple methylation and proteolysis steps, amidine macrocycle and thiazole heterocycle formation, and C-terminal decarboxylation[4–6] (Figure 1).

Previously, using gene deletion experiments and subsequent product formation analysis, only the unusual set of methyl transferases had been assigned to their function in bottromycin biosynthesis[3,4,7]. Now an order for these transformations as well as functions for the modifying enzymes have very recently been proposed based on metabolomics data of an engineered bottromycin pathway[5]. In that analysis BotP appears to be the first enzyme of the pathway to act on BotA.

BotP, shares sequence homology with a number of M17 leucine aminopeptidases (LAPs) from various organisms[3,6] (Figure S1). These metal dependent proteases hydrolyse peptide substrates with N-terminal leucine and methionine residues[8]. The function of LAPs in nature has evolved beyond ordinary roles in cell maintenance: degrading peptides released by endoproteases and the proteasome into amino acids. They are implicated in various additional biological functions, including the processing of bioactive peptides, vesicular trafficking, transcriptional regulation, mediating site-specific recombination, and as viral and toxin receptors[8,9].

As a putative LAP it is predicted that BotP facilitates the removal of methionine from the N-terminus of BotA[3]. Here we report the first biochemical and structural characterization of a PTM enzyme from the bottromycin biosynthetic pathway. The crystal structures of apo BotP and of BotP in complex with Mn^{2+} allowed us to build a BotP/substrate peptide model and determine the BotP residues involved in substrate recognition. Incubation of BotP with recombinantly produced BotA shows that this enzyme is responsible for the removal of the N-terminal methionine of BotA. The predictions based on our enzyme/substrate model were then tested in biochemical assays using peptide substrates.

Results and Discussion

Overall structure of BotP

BotP was purified as described in the materials and methods section and subjected to crystallisation trials using commercially available sparse-matrix screens. Crystals grew after three days in a number of conditions, but were too small to yield good diffraction. Following optimization, the best crystals were selected and a data set was collected at Diamond to 1.76 Å

[a] G. Mann[+], Dr B. Nardone, Prof N. J. Westwood
School of Chemistry and Biomedical Sciences Research Centre
University of St Andrews
North Haugh, St Andrews KY16 9ST (UK)
E-mail: jesko.koehnke@helmholtz-hzi.de
[b] Dr L. Huo[+]
Roger Adams Laboratory 156
University of Illinois at Urbana-Champaign
600 South Mathews Avenue
Urbana, Illinois 61801 (USA)
[c] Dr J. Koehnke
Workgroup Structural Biology of Biosynthetic Enzymes, Helmholtz Institute for Pharmaceutical Research, Helmholtz Centre for Infection Research
Saarland University
Saarbrücken, Saarland 66123, (Germany)
[d] Dr J. Vendome
Department of Biochemistry and Molecular Biophysics
Columbia University
New York, NY, 10032 (USA)
[e] Dr J. Vendome
Howard Hughes Medical Institute,
Columbia University,
New York, NY, 10032 (USA)
[f] Prof R. Müller
Department of Microbial Natural Products, Helmholtz Institute for Pharmaceutical Research, Helmholtz Centre for Infection Research
Saarland University
Saarbrücken, Saarland 66123, (Germany)
[+] These authors contributed equally to this work.

Supporting information for this article is given via a link at the end of the document.

(PDB 5LHJ). The structure was determined using molecular replacement (ensemble of multiple search models). The data collection and refinement statistics can be found in Table 1. The crystal contained one monomer in the asymmetric unit, which like other M17 LAPs is one subunit of a hexamer (Figure 2A). Analysis with *PISA* (software that enables the exploration of macromolecular interfaces)[10] suggests this hexameric assembly to be biologically relevant, which is consistent with previous observations in homologous structures[9,11,12]. A BotP monomer consists of a small N-terminal domain (residues 35-163), and a larger pseudo-spherical C-terminal catalytic domain (residues 164-499), creating a characteristic 'comma' shape (Figure 2B). The overall structure of BotP is highly similar to other M17 LAPs, and structural comparison with the recently characterized XoLAP[11] (PDB ID 3JRU) shows a C_α root mean square deviation (RMSD) of 1.61 Å over 339 residues. Superimposing the two structures in PyMOL reveals that while the two C-terminal domains are highly similar, the smaller N-terminal domains show slightly more deviation, which is a common observation within the protein family (Figure S2).

Putative catalytically important residues of BotP (based on alignments with other LAPs) are completely conserved in both sequence and structure (Figure S1). Within this cluster of active site-residues a chloride ion is in place of the bicarbonate ion commonly found in LAPs. However, the two divalent metal ions observed in LAPs are absent in this structure despite conservation of all the ligating residues (Figure S3).

Biochemical characterization of BotP

Recombinantly produced precursor peptide BotA (100 μM) was incubated with BotP (5 μM) at 37 °C overnight and proteolysis was monitored by LC-MS (Figure S4). No activity could be detected, which we believed to be a result of the absence of metal ions (as seen in the structure). Typical metals found in active LAPs include Zn^{2+}, Mn^{2+} Co^{2+} and Mg^{2+} ions[8,13]. The proteolysis reaction was repeated with a truncated version of BotA in the presence of 100 μM of each metal ion and reaction progress was monitored over time using LC-MS (Figure 3A). Addition of Co^{2+} conferred the highest activity with complete substrate turnover observed after just 1 h (Figure 3A, S4). BotP was less active in the presence of Mn^{2+}, processing ~ 90 % of the substrate in 12 h, while almost no activity was detected with Mg^{2+} and Zn^{2+} ions (Figure 3A).

Metal binding of BotP

Given the partial and full restoration of activity in the presence of Mn^{2+} and Co^{2+} respectively we sought to determine the structures of BotP in complex with these ions. Soaking optimized BotP apo crystals in the presence of $MnCl_2$ was detrimental to the diffraction quality of the crystals. Consequently BotP was pre-incubated with $MnCl_2$ overnight on ice, prior to crystal screening. Crystals of putative BotP-Mn^{2+} complexes grew in conditions different to the apo crystals. Attempts to obtain a BotP-Co^{2+} complex via both crystal soaking and pre-incubation were unsuccessful. The putative BotP-Mn^{2+} crystals were back-soaked prior to freezing to remove any unbound Mn^{2+} ions. These crystals were then used in an X-ray fluorescence scan to confirm the presence of Mn^{2+} in the crystals. The recorded spectrum (Figure S5) is congruent with the presence of Mn^{2+} in the BotP-Mn^{2+} crystals. Data for these crystals was collected at the SLS at the Mn-edge and the complex structure solved using Mn-SAD (Manganese Single-wavelength Anomalous Diffraction, PDB 5LHK). As expected both putative metal binding sites were occupied with Mn^{2+} (Figure 2C). This time a bicarbonate ion was found in place of the chloride ion in the apo structure.

Substrate recognition by BotP

A common property of enzymes from RiPP natural product biosynthesis is their broad substrate tolerance, enabling the same enzymes to synthesize multiple products[14,15]. Since co-crystallization of BotP with substrate peptides or full-length BotA proved intractable due to slow crystal growth and fast enzymatic turnover, we used modeling to provide insights into substrate specificity. The hexameric assembly of BotP prevents accurate modeling of BotA beyond residue 4, which led us to model the complex of BotP with the sequence MGPV (P1-P3' in protease nomenclature (Figure 4A, S6); the enzyme pocket binding the P1 residue is referred to as S1 and so forth.). We did not find any indication that substrate residues beyond MGPV are involved in BotP binding *in silico*, with the C-terminal Val residue only marginally contributing to binding. To test this experimentally, we performed a competition assay using BotA and truncated BotA (MGPVV). BotA gets processed in the same manner but ~4-fold faster than the truncated version (Figure S4C). It could not be determined whether this difference in rate is the result of (non)-specific substrate-enzyme interactions or simply a thermodynamic effect of the substrate size. Nevertheless our model adequately addresses the substrate specificity, which primarily concerns the first three residues of the core peptide. We verified this claim by our subsequent biochemical experimentation. The long and narrow S1 pocket is very well suited to accommodate methionine residues with an extended side-chain. The P1 methionine residue makes hydrophobic contact with Thr375 and forms a hydrogen bond with Thr373 (Figure 4B). Additionally it partakes in the extensive hydrogen-bonding network involving the two Mn^{2+} ions (Figure 4B). The S1 pocket might also allow the binding of Gly, Ala and C_γ-branched amino acids. Residues branched at the C_β cannot fit into the pocket. To test this hypothesis we incubated BotP with Co^{2+} ions and peptides MGPVV (wild-type), *L*GPVV and *I*GPVV. The *L*GPVV peptide was processed slowly (compared to wild-type) and complete turnover was observed after 6 h (Figure 3B). However the *I*GPVV peptide was only partially cleaved by BotP after 12 h, indicating it is a very poor substrate. The S1' pocket is particularly narrow and the glycine forms hydrogen bonds with the carbonyl of Leu374 and the side-and main-chain of Ser376. At first glance our model would only allow for glycine residues. However, assuming a slight rotation of the BotP Asn301 side-chain, larger residues could also be accommodated including Val or Ile. We sought to test this hypothesis by attempting to cleave M*A*PVV and M*I*PVV (Figure 3C). Both changes were accepted, but cleavage progressed much faster with the Ala substitution. To probe substrate tolerance at this position further an additional 16 substrate peptides were tested (Figure S7). As expected Ser was processed as well as Ala and bulkier amino acids and those with longer side-chains were processed more slowly. A surprise was Lys in the P1' position, which still gets processed at half the rate of Ala/Ser. We believe this to be the result of Lys's extraordinarily flexible side-chain. The S2' and S3' pockets provide an interesting insight into substrate recognition. BotP residues Asn344 and Asp440 block most of the S3' pocket (Figure 4B). These residues are usually Ala and Gly residues, respectively, in other LAPs. This is consistent with P2' being a proline residue, which introduces an elbow into the substrate peptide, leading it away from the enzyme's surface. The Pro residues make hydrophobic interactions with His341, Asn344 and Asp440. Substitution of P2' Pro to Ala (MG*A*VV) was tolerated by BotP but at a rate slower compared with the wild-type sequence (Figure 3D).

Conclusions

The bottromycins are members of the ever-growing ribosomal and post-translationally modified peptide synthesis family of natural products. They are synthesized as a precursor peptide, which undergoes extensive enzymatic (and possibly non-enzymatic) post-translational modification to become the final product. At present much of the detail regarding the enzymatic transformations remains unknown. One essential modification is

the removal of the N-terminal methionine from the precursor peptide BotA. Sequence homology with a number of known leucyl aminopeptidases indicated BotP as the enzyme responsible for this modification.

Recombinant BotP isolated from *E. coli* was initially inactive due to the absence of divalent metal ions as cofactors. Addition of Mn^{2+} or Co^{2+} restored activity. Turnover was faster with Co^{2+} than with Mn^{2+}. There has been a long debate regarding the identity of the divalent metal ions bound at the active sites of LAPs[8]. While this study identifies Co^{2+} as the ion giving the highest relative level of activity, we cannot discern which metal ions (or combinations of metal ions) are preferred in the natural producer of bottromycins. Nevertheless it would seem that Co^{2+} would be a good choice for future *in vitro* studies.

Most PTM enzymes from RiPP pathways act on the leader peptide or protease recognition elements outside the core peptide. This separation of recognition from catalysis results in a large tolerance for substrate changes by the respective enzymes. In fact, the sequence of several core peptides can essentially be hypervariable. In the case of bottromycins, the absence of an N-terminal protease site outside the core peptide could be interpreted as a severe restriction on the combinatorial possibilities for engineered substrates. However, it appears that, perhaps in an effort to limit this restriction, BotP seems to have evolved to recognize and bind to just 3 residues with binding pockets S3' partially, and S4' and S5' completely, inaccessible, compared with other LAPs. Even for the binding pockets that are available, BotP is able to at least tolerate drastic single amino acid changes, although processing progresses more slowly. This may bode well for future engineering of the pathway, since BotP activity is essential to liberate the N-terminus of BotA, thus making it available for macrocyclisation. We would like to note that BotP processes its substrate significantly faster than other RiPP proteases. We believe this to be a reflection of its relative position in the biochemical cascade – normally RiPPs proteases remove the leader and it has been suggested that they are deliberately slow to avoid cleavage before the PTMs are completed. BotP has no such restrictions. In fact, by being the first enzyme of the pathway short processing times are essential for efficient bottromycin biosynthesis.

Bottromycins exhibit promising antimicrobial activity, owed to a unique molecular scaffold and a novel biological target. Their biosynthesis requires diverse chemical transformations. The better understanding of BotP as a PTM enzyme of this pathway is a first step towards structure guided and targeted compound modification *in vitro* and *in vivo* to unlock the bottromycins' full antibiotic potential.

Experimental Section

Protein cloning, expression and purification

Full-length *botP* was cloned into pEHISMBPTEV and expressed in *E. coli* BL21 DE3 cells grown in auto-induction medium at 20 °C for 48 h[16,17]. Cells were harvested by centrifugation (4000 g, 4 °C, 15 min) and resuspended in lysis buffer (500 mM NaCl, 20 mM imidazole, 20 mM Tris pH 8.0, 3 mM β-mercaptoethanol (BME)) supplemented with cOmplete EDTA-free protease inhibitor tablets (Roche) and DNase (0.4 mg g^{-1} wet cells, Sigma). Cell suspension was lysed via passage through a cell disruptor (30 kpsi, Constant Systems Ltd), and the cell debris were removed by centrifugation (40 000 g, 4 °C, 20 min). The supernatant was filtered through a 0.45 µm filter and applied to a HF-Ni-NTA (GE Healthcare) pre-equilibrated in lysis buffer. The protein was eluted in lysis buffer supplemented with extra imidazole (250 mM). The protein eluent was passed over a desalting column (16/10 GE Healthcare) into "low imidazole, low salt" buffer (150 mM NaCl, 20 mM imidazole, 20 mM Tris pH 8.0, 3 mM BME) and subsequently incubated with TEV protease at room temperature for 2 h to remove His_6-tagged-MBP. Digested protein was loaded onto a HF-Ni-NTA, and the flow through was collected. A homogenous and pure sample as obtained via passage down a Superdex 200 gel filtration column (GE Healthcare) pre-equilibrated in gel filtration buffer (150 mM NaCl, 10 mM HEPES pH 7.4, 1 mM TCEP). Protein purity was assessed by SDS-PAGE and integrity confirmed by MS.

Full-length, codon-optimized botA was constructed from synthetic primers using PCR and cloned into the pEHISSUMOTEV plasmid to introduce a TEV cleavable SUMO tag. Expression and purification were performed as described for BotP.

X-ray Crystallography

Crystals of apo-BotP were obtained in PEG 3350 (20 % (w/v)) and sodium malonate pH 7.0 (0.24 M). Crystals of BotP-Mn^{2+} complex were obtained in PEG 4000 (10 % w/v)), MES pH 6.5 (0.1 M). Diffraction data for apo-BotP and BotP-Mn^{2+} crystals were collected at Beamlines I04-1 (Diamond light source) and X06DA (Swiss Light Source), respectively. Data was processed using Xia2 and the apo structure solved using PHASER Molecular Replacement using an ensemble of multiple search models generated in Ensemblr[18–20]. The Mn^{2+}-structure was solved using PHENIX autosol with autobuild[21,22]. The models were manually rebuilt with COOT and refined using PHENIX[21,22] and Refmac5[23]. The structure was validated using *MolProbity* and all images were presented using PyMOL[24,25]. Interaction diagrams were created using Ligplot[26].

Modeling of Substrate Complex

The peptide MGPV was modeled in the catalytic pocket of the reported structure of BotP using the crystal structure of the small peptidomimetic molecule Ubenimex (a.k.a. Bestatin) bound in the catalytic site of the zinc-dependent leucine aminopeptidase from *Pseudomonas putida* ppLAP (PDB code 3H8G, chain A) as a template. Specifically, the structure of *Pseudomonas putida* ppLAP bound to Ubenimex was aligned to our structure of BotP, and the coordinates of chosen atoms of Ubenimex were used as initial position for certain P1, P1' and P2' backbone atoms. Initial coordinates for the remaining atoms of P1, P1', P2' and P3' were generated using the build internal coordinates function in Charm (version c32a2). The structure of the peptide was then minimized in the context of the BotP catalytic site, using 50 steps of steepest descent followed by 1000 steps of conjugate gradient minimization, with a position constraint of 10 kcal mol^{-1} on all BotP heavy atoms. Since two peptidomimetic inhibitors of leucine aminopeptidase, namely Ubenimex and Leucine p-nitroaminal, were previously reported to bind LAP with their N-terminus in a deprotonated form (NH_2), both the protonated (NH_3^+) and deprotonated (NH_2) forms of the MGPV peptide were modeled following the protocol described above. Consistent with what was observed for the two peptidomimetic inhibitors, the deprotonated form bound much more favorably in the BotP site, the NH2 group notably coordinating the second zinc ion. The model with a deprotonated N-terminus is presented in the article.

Peptide Synthesis

The solid-phase synthesis of the peptides was carried out on a Rink-amide PEG resin (0.45 mmol g^{-1}) purchased from Meck-Millipore. Fmoc amino acids and all other reagents were purchased from Sigma-Aldrich and were used without any further purification. Syntheses were performed manually on a 0.023 mmol scale. Amino acids were coupled using a 5-fold excess (0.12 mmol). A solution of 0.5 M HBTU (0.12 mmol, 46 mg) in DMF (1mL) was added to the Fmoc protected amino acid, followed by DIPEA (0.12 mmol, 21 µl) and the amino acid was activated for 30 sec prior to coupling. The resin was bubbled with N_2. A single treatment of 1 h was used for all amino acids. The Fmoc group was deprotected with 20 % piperidine / DMF (v/v, 1 mL) for 10 min. Couplings were checked using the ninhidrin test. The resin was washed with DMF (6 × 1 mL) at the end of each coupling. The peptidyl-resin was dried under

vacuum and the peptide was cleaved from the resin with the reagent cocktail: 81 % trifluoroacetic acid (TFA), 5 % phenol, 5 % thioanisol, 5.5 % water, 2 % dimethylsulfide, and 1.5 % ammonium iodide (2.5 mL) for 2 h.
The TFA solution containing the peptide was concentrated under vacuum to a minimal volume, added over cold Et_2O and precipitated by centrifugation. The supernatant was removed and the residue was dissolved in 20 mL of ACN/H_2O (1:1) 0.1% TFA (HPLC buffer) and lyophilized. Peptides were used for the assays without further purification.

BotP Proteolysis Reactions
Substrate peptides (100 μM) were incubated with M^{2+} (100 μM) and BotP (5 μM) at 37 °C, 200 rpm. The reactions were analyzed at the time intervals specified via LC-MS.

LC-MS
High Performance Liquid Chromatography-Mass Spectrometry (HPLC-MS) (Thermo Ultimate 3000 RSLC, coupled to a Bruker Daltonics amaZon Electrospray Ionization (ESI)-MS ion trap instrument) was operated in positive ionization mode. Compounds were separated on a Waters Acquity BEH C18 column (50 x 2.1 mm; 1.7 µm particle diameter) at a flow rate of 600 ml min^{-1} and 45 °C by a linear gradient with (A) H_2O + 0.1 % formic acid (FA) to (B) acetonitrile (ACN) + 0.1 % FA at a flow rate of 600 µl min^{-1} and 45 °C. The gradient was initiated by a 0.33 min isocratic step at 5 % B, followed by an increase to 95 % B in 9 min to end up with a 1 min flush step at 95 % B before re-equilibration with initial conditions. Detection was carried out by both diode array (DAD) and ESI-MS. Extracted ion chromatograms were generated for the expected mass +/- 0.5 *m/z*. The amount of substrate and the product were analysed using peak area.

Acknowledgements

We acknowledge use of the Diamond (beamline I04-1) and SLS (beamline X06DA) synchrotrons. JK would like to thank the University of St Andrews, which is supported by a Wellcome Trust Capital Award (086036) and the Deutsche Forschungsgemeinschaft for an Emmy Noether fellowship (KO4116/3-1) and Daniel Sauer, Dr. Hilda Sucipto and Eva Luxenburger for help with the biochemical assays and MS analysis. BN would like to thank the European Research Council (339367).

Keywords: bottromycin • leucyl-amino peptidase • RiPPs • BotP

References

[1] P. G. Arnison, M. J. Bibb, G. Bierbaum, A. A. Bowers, T. S. Bugni, G. Bulaj, J. A. Camarero, D. J. Campopiano, G. L. Challis, J. Clardy, et al., *Nat. Prod. Rep.* **2013**, *30*, 108–160.
[2] T. J. Oman, W. A. van der Donk, *Nat. Chem. Biol.* **2010**, *6*, 9–18.
[3] L. Huo, S. Rachid, M. Stadler, S. C. Wenzel, R. Müller, *Chem. Biol.* **2012**, *19*, 1278–1287.
[4] W. J. K. Crone, F. J. Leeper, A. W. Truman, *Chem. Sci.* **2012**, *3*, 3516–3521.
[5] W. J. K. Crone, N. M. Vior, J. Santos-Aberturas, L. G. Schmitz, F. J. Leeper, A. W. Truman, *Angew. Chem. Int. Ed.* **2016**, n/a–n/a.
[6] Y. Hou, M. D. B. Tianero, J. C. Kwan, T. P. Wyche, C. R. Michel, G. A. Ellis, E. Vazquez-Rivera, D. R. Braun, W. E. Rose, E. W. Schmidt, et al., *Org. Lett.* **2012**, *14*, 5050–5053.
[7] J. P. Gomez-Escribano, L. Song, M. J. Bibb, G. L. Challis, *Chem. Sci.* **2012**, *3*, 3522–3525.
[8] M. Matsui, J. H. Fowler, L. L. Walling, *Biol. Chem.* **2006**, *387*, 1535–1544.
[9] S. Dorus, E. C. Wilkin, T. L. Karr, *BMC Genomics* **2011**, *12*, 177.
[10] E. Krissinel, K. Henrick, *J. Mol. Biol.* **2007**, *372*, 774–797.
[11] J.-K. Kim, S. Natarajan, H. Park, K.-H. Huynh, S. H. Lee, J.-G. Kim, Y.-J. Ahn, L.-W. Kang, *J. Microbiol.* **2013**, *51*, 627–632.
[12] H. Kim, W. N. Lipscomb, *Biochemistry (Mosc.)* **1993**, *32*, 8465–8478.
[13] A. Kale, T. Pijning, T. Sonke, B. W. Dijkstra, A.-M. W. H. Thunnissen, *J. Mol. Biol.* **2010**, *398*, 703–714.
[14] W. E. Houssen, A. F. Bent, A. R. McEwan, N. Pieiller, J. Tabudravu, J. Koehnke, G. Mann, R. I. Adaba, L. Thomas, U. W. Hawas, et al., *Angew. Chem. Int. Ed Engl.* **2014**, *53*, 14171–14174.
[15] D. E. Ruffner, E. W. Schmidt, J. R. Heemstra, *ACS Synth. Biol.* **2014**, DOI 10.1021/sb500267d.
[16] H. Liu, J. H. Naismith, *Protein Expr. Purif.* **2009**, *63*, 102–111.
[17] F. W. Studier, *Protein Expr. Purif.* **2005**, *41*, 207–234.
[18] G. Winter, *J. Appl. Crystallogr.* **2010**, *43*, 186–190.
[19] A. J. McCoy, R. W. Grosse-Kunstleve, P. D. Adams, M. D. Winn, L. C. Storoni, R. J. Read, *J. Appl. Crystallogr.* **2007**, *40*, 658–674.
[20] X. Wang, J. Snoeyink, *IEEE/ACM Trans. Comput. Biol. Bioinform.* **2008**, *5*, 525–533.
[21] P. Emsley, K. Cowtan, *Acta Crystallogr. D Biol. Crystallogr.* **2004**, *60*, 2126–2132.
[22] P. D. Adams, P. V. Afonine, G. Bunkóczi, V. B. Chen, I. W. Davis, N. Echols, J. J. Headd, L.-W. Hung, G. J. Kapral, R. W. Grosse-Kunstleve, et al., *Acta Crystallogr. D Biol. Crystallogr.* **2010**, *66*, 213–221.
[23] G. N. Murshudov, P. Skubák, A. A. Lebedev, N. S. Pannu, R. A. Steiner, R. A. Nicholls, M. D. Winn, F. Long, A. A. Vagin, *Acta Crystallogr. D Biol. Crystallogr.* **2011**, *67*, 355–367.
[24] V. B. Chen, W. B. Arendall 3rd, J. J. Headd, D. A. Keedy, R. M. Immormino, G. J. Kapral, L. W. Murray, J. S. Richardson, D. C. Richardson, *Acta Crystallogr. D Biol. Crystallogr.* **2010**, *66*, 12–21.
[25] *The PyMOL Molecular Graphics System, Version 1.5.0.4, Schrödinger, LLC,* **n.d.**
[26] A. C. Wallace, R. A. Laskowski, J. M. Thornton, *Protein Eng.* **1995**, *8*, 127–134.

Figure 1. Bottromycin A2 is derived from a ribosomally synthesized precursor peptide BotA (black), containing a core peptide (black) and a C-terminal follower sequence (green). The precursor peptide undergoes a series of post-translational modifications to become the natural product Bottromycin A2. The genes within the gene cluster are coloured according to the modifications their gene products are proposed to catalyse[5]. The order of the modifications have been reported and include proteolysis either side of the core peptide (green), heterocyclisation of the C-terminal cysteine within the core peptide (purple) oxidation of the resultant thiazoline to thiazole (red), Cβ-methylation (dark-blue), O-methylation (light-blue), and macrocyclisation (orange). Epimerisation (pink) is likely spontaneous[5].

Figure 2. Cartoon representation of the crystal structure of BotP. A) BotP hexamer. For clarity individual monomers are colored green, yellow, cyan, pink, red and purple. B) BotP monomer depicting the characteristic 'comma' shape. The variable N-terminal domain is shown in blue and the catalytic C-terminal domain is shown in green. A chloride ion (in place of the bicarbonate ion in other LAPs) is shown as a yellow sphere. C) The active site of the BotP-Mn^{2+} complex. Conserved catalytically important residues are shown as green sticks, Mn^{2+} ions as grey spheres and bicarbonate as green sticks. Difference electron density (F_0-F_c) contoured to 3σ with phases calculated from a model that was refined in the absence of metal ions is shown as a blue isomesh.

Figure 3. A) Relative proteolysis rate of a truncated version of BotA (MGPVV) by BotP in the presence of different metal ions. Using BotP-Co^{2+} we tested different residues in the P1 (B), P1' (C) and P2' (D) position. The reactions were monitored at specific time points by LC-MS. For each time point the amount of substrate and product were determined, and the % conversion was calculated. Results for full-length BotA are analogous (Figure S3).

Figure 4. Model of substrate peptide MGPV (cyan) with BotP-Mn^{2+} (green). A) Cartoon representation. B) Ligplot representation. Hydrogen bonds and ligand bonds are shown as red dashes. Mn^{2+} ions are shown as grey spheres, the bicarbonate ion (BCT) is only shown in A since it does not interact directly with substrate or metal ions.

Table 1. Data Collection and Refinement Statistics

	BotP_apo	BotP-Mn^{2+}
Resolution range (Å)	24.22 - 1.76 (1.82 - 1.76)	47.21 - 2.32 (2.38 - 2.32)
Space group	P 63 2 2	P 63 2 2
Unit cell	152.42 152.42 100.90 90 90 120	151.51 151.51 101.19 90 90 120
Total reflections	638232 (97638)	1139364 (77380)
Unique reflections	68447 (6724)	30149 (2166)
Multiplicity	9.3 (8.9)	37.8 (35.7)
Wavelength (Å)	0.92	1.89
Completeness (%)	99.96 (99.96)	100.00 (99.90)
Mean I/sigma(I)	17.0 (3.3)	26.8 (5.9)
Wilson B-factor	22.16	21.79
R-merge	0.067 (0.543)	0.142 (0.736)
R-work	0.1816 (0.2444)	0.1762 (0.1965)
R-free	0.2000 (0.2674)	0.1897 (0.1983)
Number of non-hydrogen atoms	3821	3640
macromolecules	3358	3304
ligands	11	6
water	452	330
Protein residues	457	455
RMS(bonds)	0.008	0.008
RMS(angles)	1.32	1.27
Average B-factor	27.00	31.00
macromolecules	25.00	30.26
ligands	49.20	23.17
solvent	41.40	38.61

One crystal was used per dataset. Values in parenthesis are for the highest resolution shell. $R_{merge} = \sum_{hkl} \sum_i |I(hkl) - \langle I(hkl)\rangle| / \sum_{hkl} \sum_i I(hkl)$, where $I(hkl)$ is the intensity of an individual measurement and $\langle I(hkl)\rangle$ is the average intensity from multiple observations. $R_{work} = \sum_{hkl} \big||F_{obs}| - k|F_{calcd}|\big| / \sum_{hkl} |F_{obs}|$ (R_{free} calculated in the same manner by using 5% of the reflection data chosen randomly and omitted from the start of refinement).

Entry for the Table of Contents (Please choose one layout)

Layout 1:

FULL PAPER

BotP – essential maturation enzyme in Bottromycin synthetic pathway.

Understanding the biosynthesis of bottromycins will permit biotechnological engineering to unlock their potent pharmaceutical potential. The structural and biochemical studies of BotP are the first to be presented for the bottromycin biosynthetic enzymes

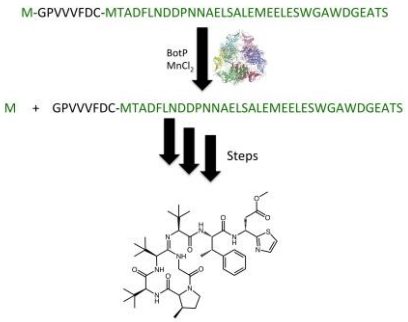

G. Mann, L. Huo, S. Adam, B. Nardone, J. Vendome, N. J. Westwood, R. Müller and J. Koehnke

Page No. – Page No.

Structure and substrate recognition of the Bottromycin maturation enzyme BotP

Figure 1

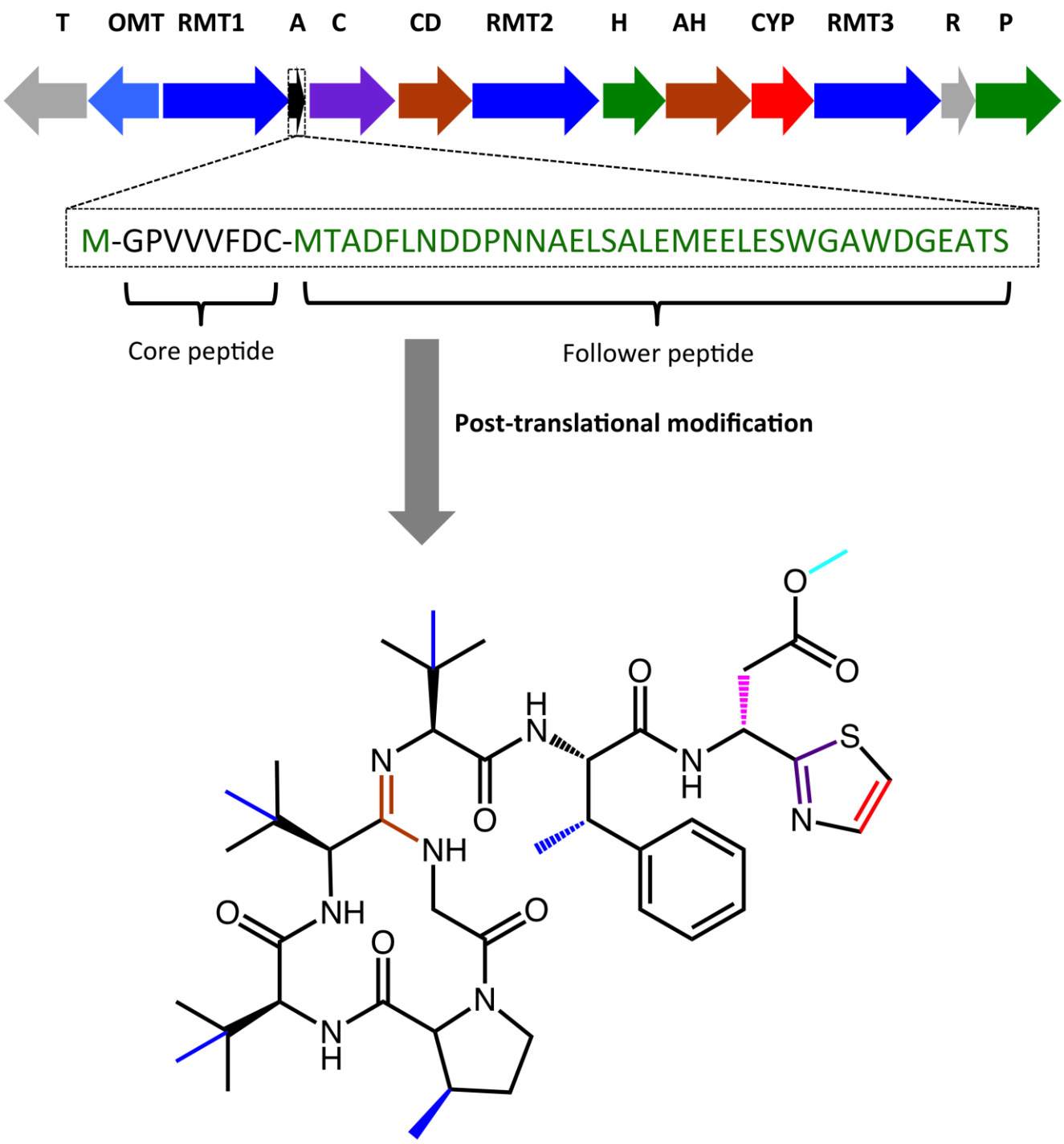

Figure 2

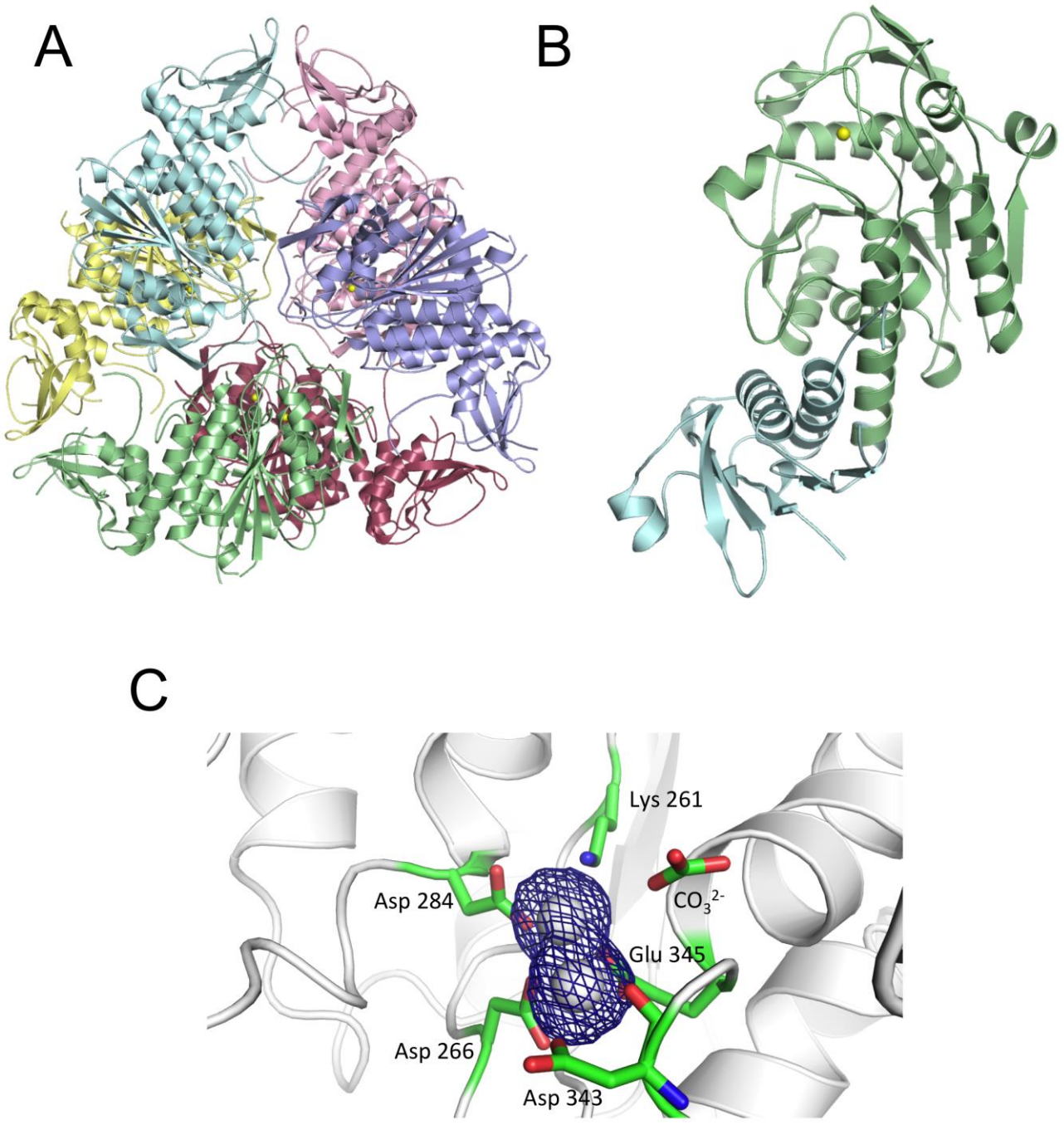

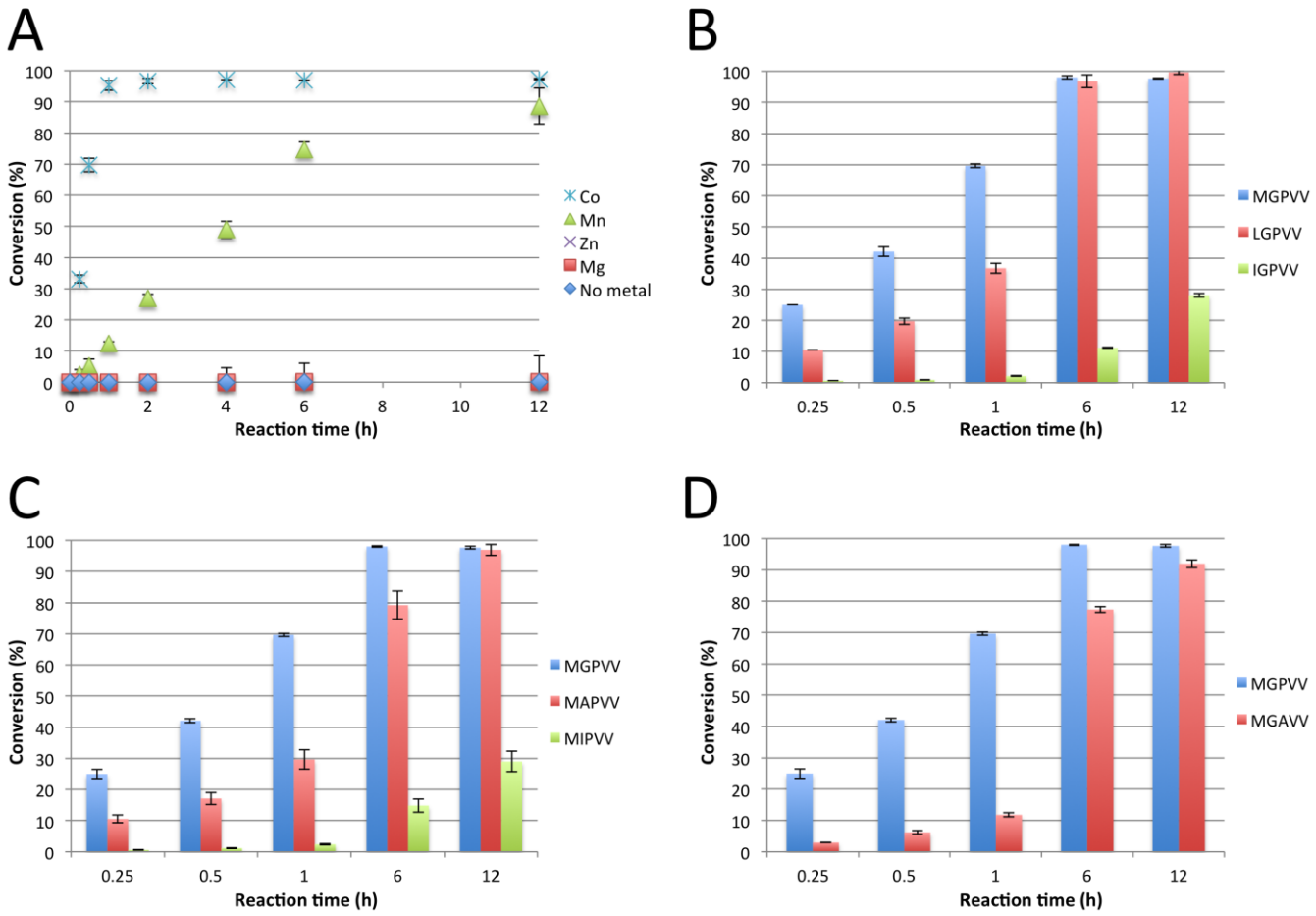

Figure 3

Figure 4

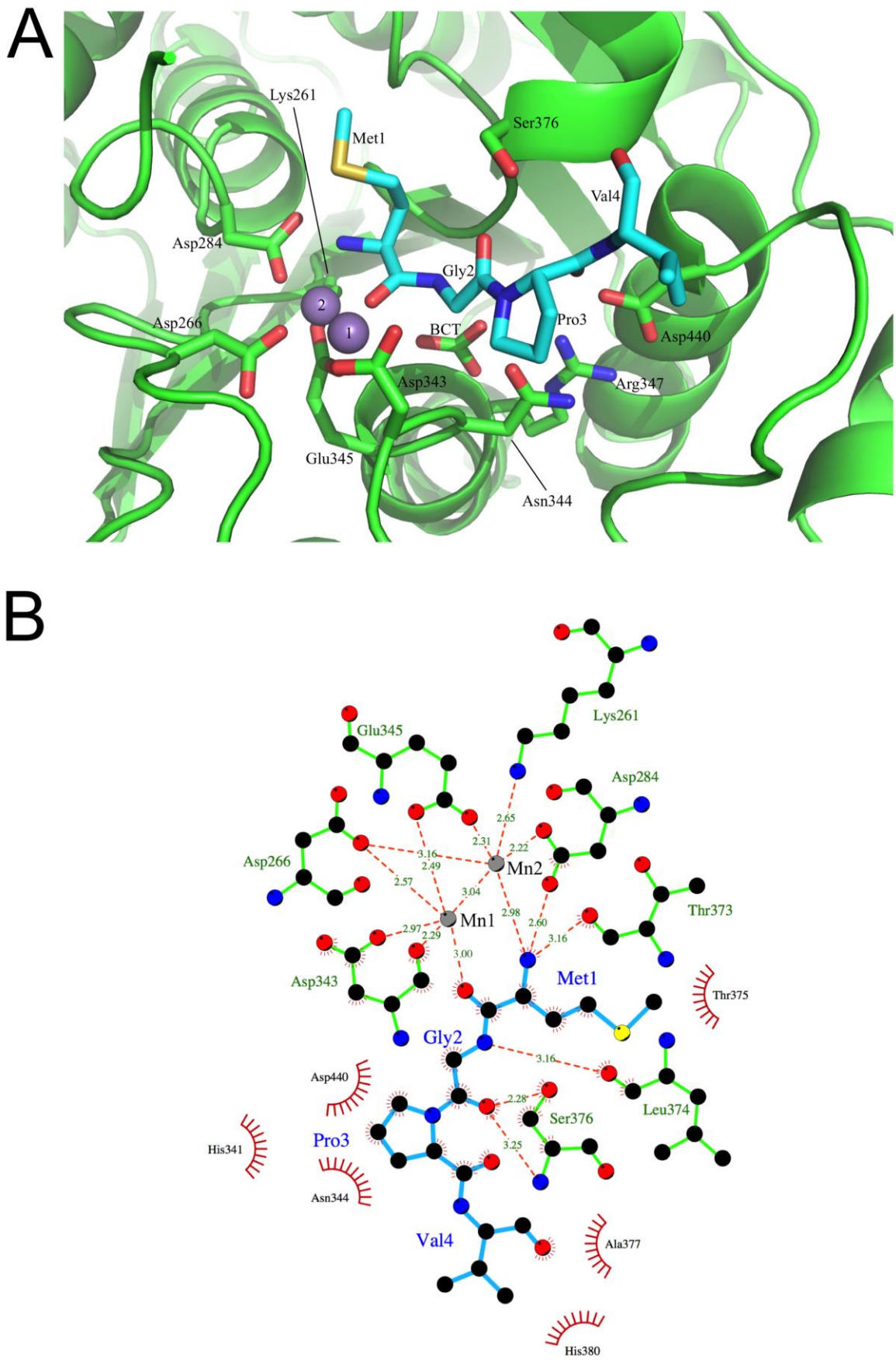

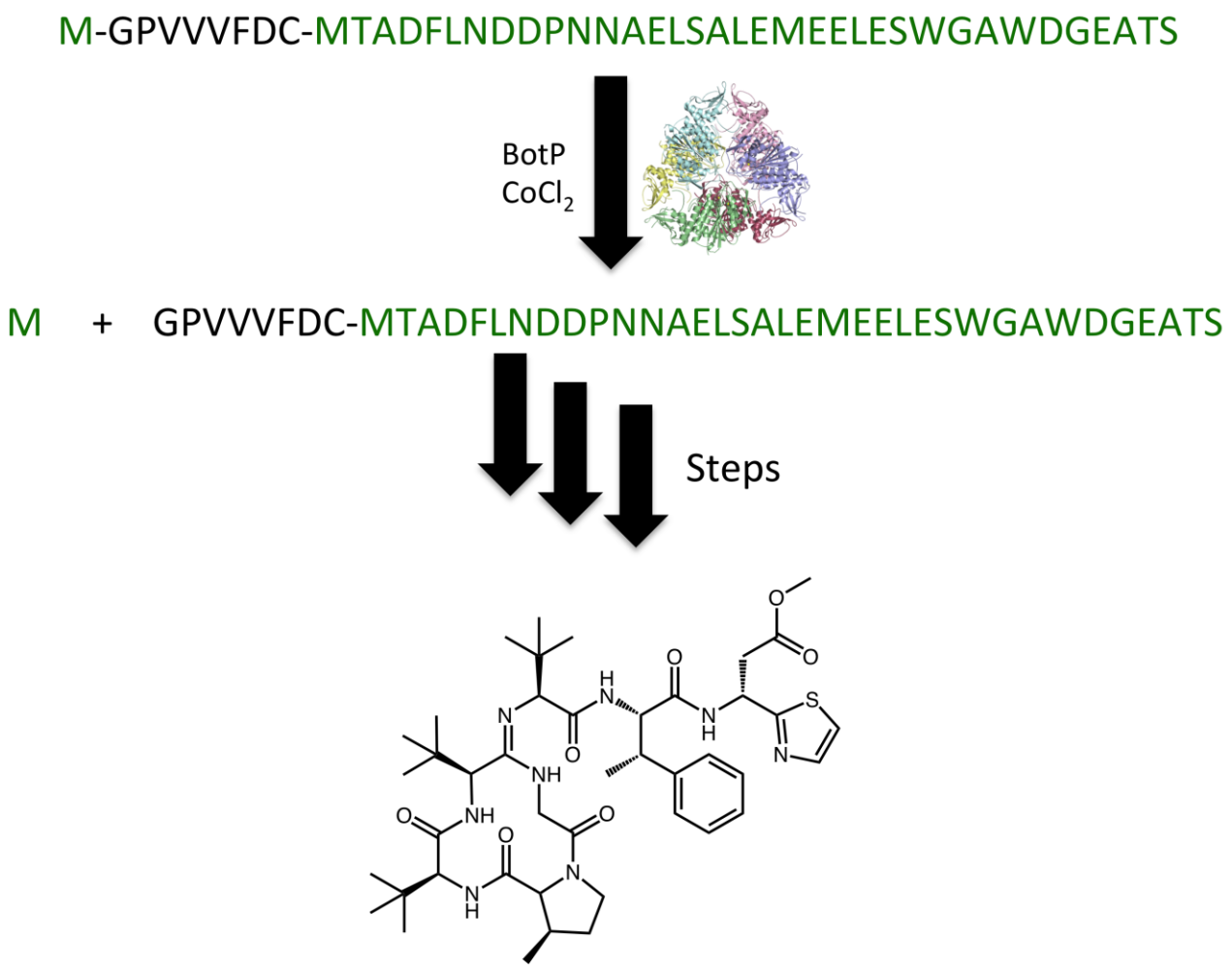

TOC